

Frustration in the coupled rattler system KOs_2O_6

J. Kuneš^{1,2,*} and W. E. Pickett¹

¹*Department of Physics, University of California, Davis, California 95616, USA*

²*Institute of Physics, Academy of Sciences of the Czech Republic, Cukrovarnická 10, 162 53 Praha 6, Czech Republic*

(Received 20 April 2006; published 18 September 2006)

Starting from *ab initio* electronic structure results we study dynamics of potassium ions in the pyrochlore superconductor KOs_2O_6 . An effective ionic Hamiltonian characterized by an on-site instability (rattler) and frustrated nearest-neighbor interaction is derived and various approximations are investigated. We show that qualitative differences in the properties of KOs_2O_6 and its analogs RbOs_2O_6 and CsOs_2O_6 arise from the relative weakness of intersite coupling, which is related to limited space for rattling in the latter compounds. We argue that the unusual physical properties of KOs_2O_6 are related to unconventional lattice dynamics rather than electronic correlations.

DOI: [10.1103/PhysRevB.74.094302](https://doi.org/10.1103/PhysRevB.74.094302)

PACS number(s): 63.20.Pw, 74.70.Dd, 63.70.+h

The phenomenon of frustration, which gives rise to much fascinating behavior, is conventionally associated with the topology of nonbipartite lattices, where nearest-neighbor (NN) interactions and global connectivity compete in the lowering of energy. The issue of rattling atoms in spacious lattice sites¹ is a separate occurrence that can also lead to a high density of low energy states (thus unusual low temperature thermodynamics) and to practical applications such as in improved thermoelectric materials.² We address a unique situation where both phenomena arise: a fourfold single-site instability leads to rattling of cations on a diamond structure sublattice where NN interactions frustrate simple ordering of the displacements. The system deals with this coupling of rattling+frustration by commensurate ordering. Such a disorder-order transition may account for the second phase transition seen in KOs_2O_6 within the superconducting state. The unusual low-energy dynamics and associated electron-phonon coupling can account for the qualitative differences in physical properties of KOs_2O_6 compared to RbOs_2O_6 and CsOs_2O_6 , all of which have essentially identical average crystal and electronic structures.

The pyrochlore-lattice-based structure with a potential to support magnetic frustration has attracted attention to the AOs_2O_6 ($A=\text{K}, \text{Rb}, \text{Cs}$) group. Unexpectedly large variation of the superconducting T_c throughout the group (from 3.3 K in CsOs_2O_6 to 9.7 K in KOs_2O_6)³⁻⁵ together with reports of anomalous nuclear spin relaxation⁶ and indications of an anisotropic order parameter⁷ in KOs_2O_6 pointed to a possibility of unconventional pairing and fueled the early experimental interest. While the issue of superconductivity remains controversial in the light of recent pressure experiments,³ unusual transport and thermodynamic properties were found in the normal state of KOs_2O_6 , which contrasts sharply with the standard metallic behavior of RbOs_2O_6 and CsOs_2O_6 .⁸⁻¹⁰

Uniquely to KOs_2O_6 within this class, the normal-state conductivity exhibits a non-Fermi-liquid behavior characterized by a concave temperature dependency down to low temperatures.^{11,12,20} The low temperature linear specific heat coefficient is estimated to be substantially larger than in RbOs_2O_6 and CsOs_2O_6 .¹² Recently an intriguing λ -shaped peak in the specific heat was observed in good quality KOs_2O_6 single-crystals indicative of a phase transition at $T_p=7$ K,¹² within the superconducting state. This observa-

tion was recently confirmed.¹¹ Notably, the peak position and shape do not change even when the superconductivity is suppressed below 7 K by an external field. Insensitivity to such a profound change of the electronic state indicates that the peak is rooted in the lattice dynamics rather than intrinsic electronic degrees of freedom.

Electronic structure investigations^{13,14} have revealed a considerable bandwidth of the $\text{Os-}5d-t_{2g}$ 12-band complex of about 3 eV which does not support the idea of local moment formation on the Os sites nor any emergence of frustration due to the pyrochlore topology of the Os sublattice, made of a three-dimensional network of vertex-sharing tetrahedra. Instead we find that a significant frustration, not magnetic but structural, takes place on the diamond sublattice occupied by K ions. We have shown previously¹³ that the symmetric (A_g) potassium phonon mode is unstable and that the energy can be lowered by several meV per alkali atom through rather large displacements of the K ions. Here we construct, based on first principles calculations, an effective potential describing S_4 symmetric displacements of K ions off their ideal diamond-lattice sites, with NN coupling leading to a highly frustrated system of displacements. Dynamical simulations for finite clusters reveal a classical ground state with complex pattern of displacements.

In Fig. 1 we show the AOs_2O_6 lattice which consists of Os on a pyrochlore sublattice, having one O atom bridging each Os NN pair. The cavities in the Os-O network are filled with alkali ions, which themselves form a diamond lattice, composed of two fcc sublattices. Using the full-potential linearized augmented-plane-wave code WIEN2K (Ref. 15) we have performed a series of calculations in which K ions move along the (111) direction: (i) the two fcc sublattices are displaced in opposite directions (symmetric A_g mode), (ii) same as (i) with the O positions allowed to relax, (iii) only one fcc sublattice is displaced. Comparing results (i) and (ii) reveals a non-negligible O relaxation only for large K displacement ξ_i (the energy vs displacement curve has slightly less steep walls when O ions are allowed to relax). Since the O relaxation effect is minor we consider the Os-O network to be rigid for the following discussion. In the rigid Os-O background coupling between potassium neighbors is essentially of Coulomb origin. Metallic screening and the pyrochlore lattice geometry with spacious channels between neighbor-

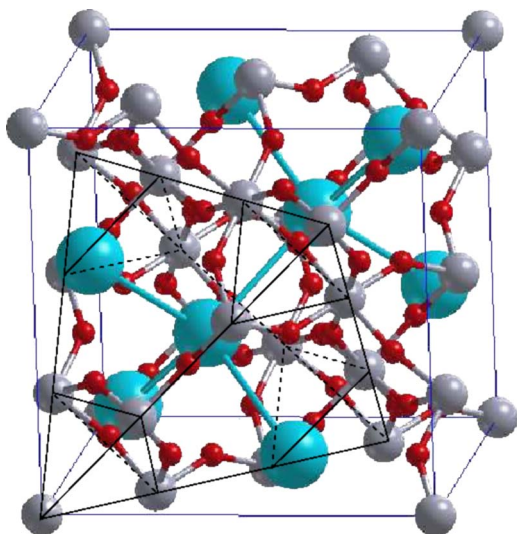


FIG. 1. (Color online) The AOs_2O_6 lattice. The atomic species are distinguished by different sizes (colors): Os is medium size (gray), O is small (red), and alkali metal ions are large (blue). The pyrochlore sublattice of Os atoms is highlighted. Notice that the alkali sublattice has a diamond structure.

ing cavities suggest NN coupling to dominate over longer range interaction. The effective Hamiltonian becomes

$$\hat{H} = \sum_i \left[\frac{p_i^2}{2M} + P_e(\xi_i) + P_o(\xi_i) \mathcal{Y}_{32}(\hat{\xi}_i) \right] + \sum_{i>j} W_{ij}(\xi_i, \xi_j), \quad (1)$$

where the first term is the on-site Hamiltonian and second describes the NN coupling (interaction). The on-site potential, which captures the essential tetrahedral local symmetry, consists of a spherical and the next nonzero term in spherical harmonic expansion (\mathcal{Y}_{lm}), while the radial dependency is described by even and odd sixth-order polynomials $P_e(\xi_i)$ and $P_o(\xi_i)$ obtained by fitting the *ab initio* data from type (iii) calculations (Fig. 2).

We have solved the quantum-mechanical single site problem by numerical integration on a real space grid (details of the calculation can be found in Ref. 16). The low energy spectrum up to 80 K (containing 20 states) is characterized by a singlet-triplet split ground state (8 K splitting) separated by a gap of about 25 K from excited states. This essential difference from the harmonic potential with singlet ground state is reflected also by a Schottkyesque anomaly in the single-site specific heat.¹⁶ The sharpness of the observed peak, however, rules out the Schottky anomaly scenario, pointing instead to a collective transformation involving intersite coupling. A particularly useful way of looking at the quasidegenerate quadruplet ground state is in terms of four symmetry related local orbitals centered in the local minima. A weak coupling of about -2 K for each pair of orbitals accounts for the singlet-triplet splitting.

Ab initio calculations¹³ revealed much less anharmonicity in the Rb and especially Cs potentials, which can be treated as a perturbation and neglected for the present purposes. Within this approximation Rb (Cs) dynamics is described by an isotropic 3D oscillator with a frequency of 44 K (61 K).

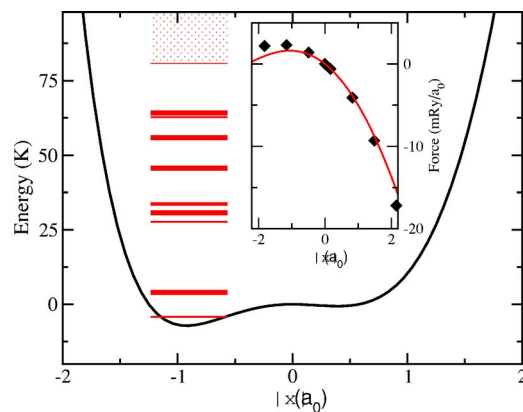


FIG. 2. (Color online) The on-site potential. The on-site potential along the NN bond direction (the NN site is in the direction of positive x axis). The vertical lines denote the eigenenergies on the same scale, the thickness represents degeneracy ranging from 1 to 3. In the inset the force acting on undisplaced ion as a function of the uniform displacement of its neighbors is shown. The symbol represents the *ab initio* data, the full line is the fit with linear pair force.

Recent analysis of specific heat data by Brühwiler *et al.*¹¹ led to a frequency of 60 K for RbOs_2O_6 , which we find a reasonable agreement given the approximations. Localized modes were previously observed in specific heat of RbOs_2O_6 and CsOs_2O_6 by Hiroi *et al.*¹⁷ The harmonic oscillator root mean square displacement is

$$\Delta = \sqrt{\langle \xi_i^2 \rangle} = \frac{1}{\sqrt{2M\omega}}, \quad (2)$$

and we obtain $\Delta_{\text{Rb}} = 0.15a_0$ ($a_0 = \text{Bohr radius}$) and $\Delta_{\text{Cs}} = 0.1a_0$ for the mean square displacement at zero temperature, which we will use below in estimation of strength of the intersite coupling.

The interaction can be obtained by following the force acting on a fixed ion when its neighbors are uniformly displaced. The simplest form of central pair force that describes reasonably well the *ab initio* data is obtained from the pair potential $V(\mathbf{r}_1, \mathbf{r}_2) = A|\mathbf{r}_{12}| + \frac{B}{2}|\mathbf{r}_{12}|^2$ (\mathbf{r}_j are ion coordinates). In Fig. 2 (inset) we show the first principles force together with the model fit, the values $A = -88 \text{ mRy}/a_0$ and $B = 7.9 \text{ mRy}/a_0^2$ are essentially the same for all three oxides. As expected from its electrostatic origin the pair force is repulsive for admissible values of r . Using the electrostatic force $-\frac{1}{r^2}$ instead of an *ad hoc* Taylor expansion, the force in Fig. 2 would not crossover to the positive values, but only reach zero for zero displacement. The observed behavior is qualitatively consistent with faster decay of the interaction due to screening. The interaction $W_{ij}(\xi_i, \xi_j)$ between ions at sites \mathbf{R}_i and \mathbf{R}_j is obtained after subtraction of contributions accounted for in the on-site potential

$$W_{ij}(\xi_i, \xi_j) = V(\mathbf{R}_i + \xi_i, \mathbf{R}_j + \xi_j) - V(\mathbf{R}_i, \mathbf{R}_j + \xi_j) - V(\mathbf{R}_i + \xi_i, \mathbf{R}_j) + V(\mathbf{R}_i, \mathbf{R}_j). \quad (3)$$

The result is a directional (non-central) potential, whose dipolar form becomes clear in the small displacement limit

$$\tilde{W}_{ij}(\xi_i, \xi_j) \approx A \frac{(\mathbf{R}_{ij} \cdot \xi_i)(\mathbf{R}_{ij} \cdot \xi_j)}{R_{ij}^3} - \left(\frac{A}{R_{ij}} + B \right) \xi_i \cdot \xi_j. \quad (4)$$

We start the discussion of NN coupling in the simpler quasiharmonic case (RbOs_2O_6 and CsOs_2O_6). Small mean displacements justify the use of a dipolar approximation (4) to estimate the interaction energy. Using the Schwarz inequality $|\langle \xi_i, \xi_j \rangle|^2 \leq \langle \xi_i^2 \rangle \langle \xi_j^2 \rangle$ the interaction energy per site for a two-site problem has the following upper bound:

$$|\langle \tilde{W} \rangle| \leq \left(\frac{|B|}{2} + \left| \frac{A}{R} + B \right| \right) \Delta^2, \quad (5)$$

yielding 23 and 10 K for Rb and Cs, respectively. Going one step further and considering the problem of four sites connected to their common neighbor the upper bound is reduced for purely geometrical reasons to 16 and 7 K, respectively. Smallness of the interaction energy in comparison to the Einstein frequencies and the singlet character of the on-site ground state lead to the conclusion that the Rb and Cs dynamics is essentially local.

The peculiarity of KOs_2O_6 . KOs_2O_6 presents the *opposite limit* of extreme anharmonicity, leading to quasidegeneracy of the ground state and large spatial fluctuations, together with important intersite coupling. In the following we evaluate the matrix elements of W in the basis of products $|\alpha\rangle$ of the on-site eigenstates. The basis of local orbitals for the ground state quadruplet has an advantage of keeping the Hamiltonian in quasidiagonal form by maximizing the diagonal terms $\langle \alpha\beta | W | \alpha\beta \rangle$ and minimizing the leading off-diagonal contributions $\langle \alpha\beta | W | \alpha\gamma \rangle$. Moreover there is a natural one-to-one mapping between the local orbitals and NN bonds, namely we denote an orbital and a bond with the same index if the orbital represents displacement in the direction of the bond. Due to the symmetry there are only four independent diagonal matrix elements, which can be expressed in the form (in K):

$$\langle \alpha\beta | W_R | \alpha\beta \rangle = -324\delta_{\alpha\beta} + 742\delta_{\alpha R}\delta_{\beta R} - 301(\delta_{\alpha R} + \delta_{\beta R}) + 147, \quad (6)$$

where both the bond index R and the orbital indices α, β run from 1 to 4. These numbers can be understood in terms of the approximate formula (4), taking into account the inversion symmetry about the bond center. The relevant off-diagonal terms yield about 15 K (additional 2 K comes from the on-site Hamiltonian). The off-diagonal terms also provide coupling to products including excited states with the largest ones being about 1/3 of the corresponding energy difference, providing thus small but non-negligible quantum mechanical coupling.

Origin of frustration. Building a lattice model from bonds (6) helps one to understand the frustrated nature of the present system. Although it is not justifiable to neglect the excited states completely, they will only renormalize the parameters without changing the four-state form of the Hamiltonian in the low energy sector. Building a lattice Hamiltonian from the bonds (6), using the fact that the third term yields a constant when summed over the bonds, we get an expression

$$H = \sum_{ij} (a\delta_{\alpha\beta}^j + b^\infty \delta_{\alpha R(ij)}^j \delta_{\beta R(ij)}^j) + H_{\text{on-site}}. \quad (7)$$

The first term of Eq. (7) is the classical Potts Hamiltonian,¹⁹ $\delta_{\alpha\beta}^j$ yields 1 when the neighboring sites i, j are occupied by the same state and zero otherwise. In the second term $R(ij)$ is an index of the bond between sites i and j , $\delta_{\alpha R(ij)}^j$ yields 1 if orbital on site i corresponds to displacement in the direction of the bond ij and zero otherwise. The bare values of parameters a and b are -162 and 371 K, respectively. Since the second term describes states whose energy is above the already neglected excited states it is consistent to rule these states out by putting b equal to $+\infty$. The second term thus becomes a constraint on admissible configurations and introduces frustration into the system. The leading quantum mechanical correction $H_{\text{on-site}}$, the bare value of which is an order of magnitude smaller than a , describes tunneling between the local orbitals. Filling the lattice such that we minimize the contribution of an arbitrary first site (only three bonds can yield a due to the constraint) one can readily see that an arrangement with the same energy cannot be placed on the neighboring sites. Unlike in the case of geometrical frustration of NN antiferromagnets no odd-length loops are necessary to produce frustration. In fact the situation here is more related to dipolar magnets¹⁸ as suggested by Eq. (4). While we cannot make conclusions about the degeneracy of the ground state, the frustrating constraint is expected to reduce the transition temperature below the energy scale defined by parameter a .

Dynamical simulations. While the effective Hamiltonian (7) can be useful for investigating general features of the phase transition and is well suited for analytical approach, in the rest of this paper we pursue a separate, purely numerical approach to probe aspects of the ordering that we anticipate at T_p . Addressing this question in full generality is very difficult. Insight can be gained by minimizing the potential energy, i.e., pursuing the classical (large mass M) limit, for finite clusters with periodic boundary conditions. This is still a formidable computational task due to a large number of local minima. To approach and possibly reach the global minimum we have used a damped molecular dynamics combined with simulated annealing. In particular we have integrated the classical equation of motion

$$M \frac{d^2 \xi}{dt^2} = \mathcal{F}(\xi) - \beta(T) \frac{d\xi}{dt} + \mathcal{G}(T), \quad (8)$$

where \mathcal{F} is the actual force, the $\beta(T) \propto \sqrt{T}$ is a friction parameter, and $\mathcal{G}(T)$ is a Gaussian random vector with half-width proportional to T . The effective temperature T was successively reduced $T_i = \epsilon T_{i-1}$ ($\epsilon < 1$) until a minimum was reached.

The minimum of the $1 \times 1 \times 1$ (single primitive cell) cluster can be described as parallel displacement of all ions along one of the bond directions with different displacement values ($1.54a_0$ toward the NN site and $1.24a_0$ away from the NN site) on the two sublattices (the global minimum is, of course, degenerate with respect to the sublattice exchange). The ordering on a $2 \times 2 \times 2$ cluster is characterized by uni-

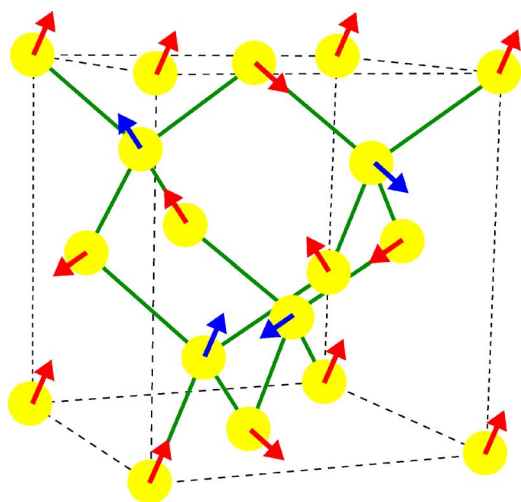


FIG. 3. (Color online) Minimum energy configuration for the $2 \times 2 \times 2$ cluster. Different shades (colors, red and blue) correspond to the two fcc sublattices, solid (green) lines mark the NN bonds. (Note that the same displacements for sites on the same edge of the cube are not enforced by the boundary conditions.)

form displacements along different bonds as shown in Fig. 3. The minima for $3 \times 3 \times 3$ and larger clusters are difficult to understand in real space since the displacements are neither uniform nor limited to bond directions. Nevertheless, common features include a small net displacement per sublattice (less than $0.1a_0$) and a (very large) average displacement of $2.0a_0$ per site with a standard deviation of about $0.3a_0$. The magnitude of the displacements is likely to be overestimated somewhat due to neglect of the kinetic energy, the effect of which can be qualitatively visualized as replacing the point particles with probability density clouds. Moreover Fourier transform of the displacement vectors $\xi_\alpha(\mathbf{R}_i)$,

$$S_\alpha(\mathbf{q}) = \frac{1}{N} \sum_i \exp(i\mathbf{q} \cdot \mathbf{R}_i) \xi_\alpha(\mathbf{R}_i), \quad (9)$$

revealed that there are only a few nonvanishing q components for each cluster size. Even with the lowest cooling rate we were not able to obtain the minimum for the $5 \times 5 \times 5$ cluster unambiguously, which strongly suggests that periodicity of 5 unit cells is not commensurate with the ordering tendencies in the system. The results are summarized in Table I. Fourier transforms are characterized by two or three dominant components with $(2/3, 2/3, 0)$ and $(1/2, 1/2, 1/2)$ appearing whenever allowed by the cluster size. Comparison of the minimum energies for different clusters indicates that beyond $3 \times 3 \times 3$ the energetics becomes very flat while the ordering wave vectors are sensitive to boundary conditions. The absolute value of this energy has no relevance for low energy scale of the ordering transition, but its convergence indicates that minimum energy is being reached.

Summary. Our results provide a picture of potassium dynamics in KO_2O_6 governed by an effective Hamiltonian characterized by an unusually soft and broad local potential, which allows for large excursions of K ions resulting in significant and frustrating NN coupling. To address the question

TABLE I. Minimum potential energy and the dominant Fourier components (only one member of $\pm\mathbf{q}$ pair is shown) for the ground states of clusters of different size (in brackets). The vectors are in the units of $\frac{2\pi}{a}$, where $a=10.101 \text{ \AA}$.

Cluster size	E (mRy)	Largest $ S(q) $ for
$1 \times 1 \times 1$ (2)	-1.99	
$2 \times 2 \times 2$ (16)	-17.11	$(1,0,0), (0,1,0), (0,0,1)$
$3 \times 3 \times 3$ (54)	-18.01	$(-\frac{2}{3}, 0, \frac{2}{3}), (\frac{2}{3}, 0, \frac{2}{3})$
$4 \times 4 \times 4$ (128)	-18.11	$(\frac{1}{2}, \frac{1}{2}, -\frac{1}{2}), (-\frac{1}{4}, \frac{1}{4}, \frac{3}{4}), (\frac{1}{4}, \frac{3}{4}, \frac{1}{4})$
$6 \times 6 \times 6$ (432)	-18.20	$(0, -\frac{2}{3}, \frac{2}{3}), (-\frac{1}{2}, \frac{1}{2}, \frac{1}{2}), (\frac{1}{2}, \frac{1}{6}, \frac{5}{6})$

of ordering tendencies we have used classical simulations for finite clusters which provide a complicated but distinct pattern with multiple- q ordering and large displacements. Since the purely numerical model is not well suited for addressing general questions concerning the phase transition and for understanding the essence of the present physics we have also proposed an analytic model with only a few parameters. This model is formally a three-dimensional ferromagnetic four-state Potts model with an additional constraint on possible configurations. While the unconstrained model is known to exhibit a first order mean-field-like phase transition,¹⁹ the constraint cannot be relieved in a simple way by the system and is likely to change behavior of the model.

Our calculations suggest a natural explanation for the second peak observed in the specific heat of KO_2O_6 (Ref. 12) as a phase transition of the potassium sublattice to supercell order. Anomalies of low temperature electronic properties such as non-Fermi-liquid conductivity and large linear specific heat coefficient¹² can be explained as a consequence of atomic motion, which does not freeze down to the ordering transition at 7 K. We point out that large excursions of the K ion should affect the NMR measurements due to quadrupolar interaction and might be responsible for observed anomalies.⁶ The dynamics of Rb and Cs ions is very different: the larger ionic radii give rise to significantly smaller spatial fluctuations and higher characteristic frequencies, and this distinction in turn negates the intersite interaction, leaving a simple quasiharmonic local mode. This result of our first principle calculations fits well with the observed specific heat and conductivity.^{11,17}

If it proves possible, synthesis of $\text{K}_x\text{Rb}_{1-x}\text{Os}_2\text{O}_6$ will provide a means of introducing “vacancies” into the model Hamiltonian (7), since the Rb sites would be normal oscillators. The combination of single-site rattling and frustrating NN coupling, facilitated by “fine-tuning” of the potassium ionic radius to the size of osmium-oxygen cage, provides a different physical system, which exhibits a phase transition at low temperature.

We acknowledge discussions with R. R. P. Singh and R. Seshadri, and communication with Z. Hiroi, M. Brühwiler, and B. Batlogg. J.K. was supported by DOE Grant No. FG02-04ER 46111 and Grant No. A1010214 of the Academy of Sciences of the Czech Republic, and W.E.P was supported by National Science Foundation Grant No. DMR-0421810.

- *Present address: Theoretical Physics III, Center for Electronic Correlations and Magnetism, Institute for Physics, University of Augsburg, D-86135 Augsburg, Germany.
- ¹V. Keppens, D. Mandrus, B. C. Sales, B. C. Chakoumakos, P. Dai, R. Coldea, M. B. Maple, D. A. Gajewski, E. J. Freeman, and S. Bennington, *Nature (London)* **395**, 876 (1998).
- ²B. C. Sales, D. Mandrus, and R. K. Williams, *Science* **272**, 1325 (1996).
- ³T. Muramatsu, N. Takeshita, C. Terakura, H. Takagi, Y. Tokura, S. Yonezawa, Y. Muraoka, and Z. Hiroi, *Phys. Rev. Lett.* **95**, 167004 (2005).
- ⁴S. Yonezawa, Y. Muraoka, Y. Matsushita, and Z. Hiroi, *J. Phys. Soc. Jpn.* **73**, 819 (2004), see also Ref. 20; M. Brühwiler, S. M. Kazakov, N. D. Zhigadlo, J. Karpinski, and B. Batlogg, *Phys. Rev. B* **70**, 020503(R) (2004).
- ⁵S. Yonezawa, Y. Muraoka, and Z. Hiroi, *J. Phys. Soc. Jpn.* **73**, 1655 (2004).
- ⁶K. Arai, J. Kikuchi, K. Kodama, M. Takigawa, S. Yonezawa, Y. Muraoka, and Z. Hiroi, cond-mat/0411460 (unpublished).
- ⁷A. Koda, W. Higemoto, K. Ohishi, S. R. Saha, R. Kadono, S. Yonezawa, Y. Muraoka, and Z. Hiori, *J. Phys. Soc. Jpn.* **74**, 1678 (2005).
- ⁸R. Khasanov, D. G. Eshchenko, J. Karpinski, S. M. Kazakov, N. D. Zhigadlo, R. Brütsch, D. Gavillet, D. Di Castro, A. Shengelaya, F. La Mattina, A. Maisuradze, C. Baines, and H. Keller, *Phys. Rev. Lett.* **93**, 157004 (2004).
- ⁹T. Schneider, R. Khasanov, and H. Keller, *Phys. Rev. Lett.* **94**, 077002 (2005).
- ¹⁰K. Magishi, J. L. Gavilano, B. Pedrini, J. Hinderer, M. Weller, H. R. Ott, S. M. Kazakov, and J. Karpinski, *Phys. Rev. B* **71**, 024524 (2005).
- ¹¹M. Brühwiler, S. M. Kazakov, J. Karpinski, and B. Batlogg, *Phys. Rev. B* **73**, 094518 (2006).
- ¹²Z. Hiroi, S. Yonezawa, T. Muramastu, J. Yamaura, and Y. Muraoka, *J. Phys. Soc. Jpn.* **74**, 1682 (2005), see also Ref. 20; M. Brühwiler, S. M. Kazakov, J. Karpinski, and B. Batlogg, *Physica B* **378-380**, 880 (2006).
- ¹³J. Kuneš, T. Jeong, and W. E. Pickett, *Phys. Rev. B* **70**, 174510 (2004).
- ¹⁴R. Saniz, J. E. Medvedeva, L. H. Ye, T. Shishidou, and A. J. Freeman, *Phys. Rev. B* **70**, 100505(R) (2004).
- ¹⁵P. Blaha, K. Schwarz, G. K. H. Madsen, D. Kvasnicka, and J. Luitz, WIEN2K, *An Augmented Plane Wave + Local Orbitals Program for Calculating Crystal Properties* (Karlheinz Schwarz, Technische Universität Wien, Wien, 2001).
- ¹⁶J. Kuneš and W. E. Pickett, *Physica B* **378-380**, 898 (2006).
- ¹⁷Z. Hiroi, S. Yonezawa, T. Muramastu, J. Yamaura, and Y. Muraoka, *J. Phys. Soc. Jpn.* **74**, 1255 (2005), see also Ref. 20.
- ¹⁸S. J. White, M. R. Roser, J. Xu, J. T. van der Noordaa, and L. R. Corruccini, *Phys. Rev. Lett.* **71**, 3553 (1993).
- ¹⁹F. Y. Wu, *Rev. Mod. Phys.* **54**, 235 (1982).
- ²⁰Z. Hiroi, S. Yonezawa, J. Yamaura, T. Muramatsu, Y. Matsushita, and Y. Muraoka, *J. Phys. Soc. Jpn.* **74**, 3400 (2005).